The Korean Journal of Ceramics, **4** [2] 156 - 161 (1998)

A Thermogravimetric Study of the Non-stoichiometry of Iron-Doped Nickel Oxide $(Ni_{1-x}Fe_x)_{1-\delta}O$

Kunt N. Krafft and Manfred Martin*

Institute of Physical Chemistry and Electrochemistry, University of Hannover, Callinstr.3-3a, D-30167 Hannover, Germany
**Institute of Physical Chemistry, Darmstadt University of Technology, Petersenstr. 20, D-64287 Darmstadt, Germany*
(Received October 2, 1997)

We have measured changes of the non-stoichiometry, $\Delta\delta$, in Fe-doped nickel oxide $(Ni_{1-x}Fe_x)_{1-\delta}O$, by thermogravimetry for four iron fractions, x=0.01, 0.031, 0.057 and 0.10, and three temperatures, T=1273, 1373 and 1473 K. The obtained data can be modelled by a defect structure in which substitutional trivalent iron ions, $Fe_{Ni}^{\cdot}$, are compensated by cation vacancies, V_{Ni}'', and (4:1)-clusters. These clusters consist of tetravalent interstitial iron, $Fe_i^{\cdot\cdot}$, surrounded tetrahedrally by four cation vacancies and are four times negatively charged.

Key words : Non-stoichiometry, Iron-doped nickel oxide, Thermogravimetry, Defect structure, Defect cluster

I. Introduction

Iron-doped nickel oxide, $(Ni_{1-x}Fe_x)_{1-\delta}O$, belongs to the class of monoxides of the iron-row which crystallize in the NaCl-structure and are non-stoichiometric compounds. Within the binary oxides of these compounds, wüstite, $Fe_{1-\delta}O$, exists only with a non-stoichiometry between 5 and 15%.[1] In contrast, the stability field of manganosite, $Mn_{1-\delta}O$, extends from the nearly stoichiometric composition, δ=0, up to $\delta \approx 20\%$.[2] In $Co_{1-\delta}O$ the non-stoichiometry reaches only about 1%[3] and $Ni_{1-\delta}O$ has the lowest deviation from stoichiometry with a maximum value of about 0.1%.[4] However, by doping, e.g. with iron, the non-stoichiometry may be increased even in NiO. In the doped oxide, $(Ni_{1-x}Fe_x)_{1-\delta}O$, δ depends on temperature, T, oxygen activity, a_{O_2}, and the fraction of iron, x. Using a coulometric titration cell for oxygen ions Schneider and Schmalzried[5] have measured changes of δ as a function of x and a_{O_2}. However, due to experimental limitations they could perform their measurements only for temperatures below 1303 K. In order to investigate δ in a larger part of the stability field of Fe-doped NiO we have performed high temperature thermogravimetric measurements where changes of δ with varying a_{O_2} at constant x and T were determined The phase diagram of the system Ni-Fe-O and the stability field of Fe-doped NiO, $(Ni_{1-x}Fe_x)_{1-\delta}O$, in which the experiments were performed are shown in Fig. 1.[5]

II. Experiments

1. Sample Preparation

Dense, polycrystalline samples of $(Ni_{1-x}Fe_x)_{1-\delta}O$ were prepared as follows. NiO powder was prepared by gel-precipitation of carbonate from aqueous nickel nitrate (p.a. Merck) and subsequent decomposition through annealing. Then powders of NiO, hematite Fe_2O_3 (p.a. Ventron) and iron (p.a. Merck) were mixed in appropriate ratios and wet ball milled in acetone. After drying, the powder mixture was compacted isostatically into cylindrical form (8 mm diameter, 4-8 mm height) and sintered at 1273 K in a gas atmosphere of 1% CO and 99% CO_2. After 2 days the samples were cooled to room temperature as fast as possible and then analysed concerning their composition by electron microprobe analysis.

2. Thermogravimetric Measurements

The measurements were performed at the Institute of Physical Chemistry and Electrochemistry, University of Hannover in a high temperature symmetric microbalance described in detail in ref.[6]. In the sample holder made of alumina, the prepared samples were placed on three very thin alumina tips to minimize reaction between the sample and the sample holder. During the measurements the sample holder and an identical counterbalance are hanging at long platinum wires at the two arms of the symmetric microbalance into a symmetric twin-furnace. Both sides of the furnace were kept at identical temperatures ($\pm$2 K). The oxygen activities in both sides were established by flowing gas mixtures of CO_2 and CO or CO_2 and air and monitored by electrochemical cells with CaO-stabilized zirconia as electrolyte. To keep the noise level low (about 1 μg) the total pressure was kept at 0.25 to 0.4 bar. The measurements were carried out in the temperature range of 1273 K to 1473 K. At each temperature investigated, the oxygen activity was varied as far as permissible within the sta-

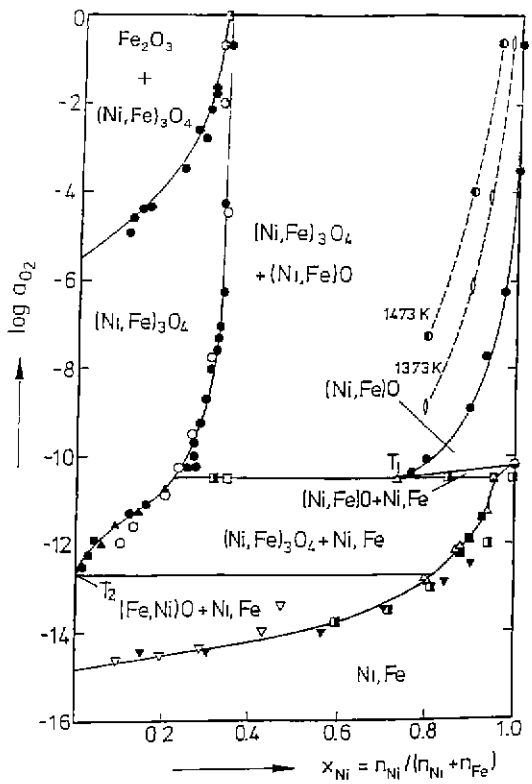

Fig. 1. Phase-diagram of the system Ni-Fe-O at T=1273 K and stability field of Fe-doped NiO, $(Ni_{1-x}Fe_x)_{1-\delta}O$, at T=1273, 1373 and 1473 K.[5]

bility range of the respective sample (see Fig. 1). The activity changes were performed by switching between several gas mixtures and the mass changes of the sample occuring thereafter were recorded. All mass changes were measured relative to the mass of the sample in equilibrium with the reference gas used.

3. Experimental Results

The measurements were carried out with four samples of different compositions, x=1.0, 3.1, 5.7 and 10 at% Fe, at temperatures of 1273, 1373 and 1473 K. The mass changes, Δm, of the sample relative to a reference point chosen for each temperature investigated were measured as a function of the oxygen activity, ao_2. After an ao_2-jump we observed extremely long relaxation times (up to 48 hours) which are probably due to slow demixing processes of Ni and Fe caused by the transient oxygen potential gradient in the sample and subsequent re-equilibration of Ni and Fe. The observed mass changes are converted to changes of the non-stoichiometry, $\Delta\delta$, with the help of the following oxidation reaction.

$$a_{n-1}(Ni_{1-x}Fe_x)_{1-\delta_{n-1}}O+\frac{1}{2}b_nO_2(g)\Rightarrow a_n(Ni_{1-x}Fe_x)_{1-\delta_n}O \qquad (1)$$

Here a_{n-1}, is the mol number and δ_{n-1}, the non-stoichiometry of the sample before the nth activity change, b_n is the mol number of consumed oxygen, and a_n and δ_n are the

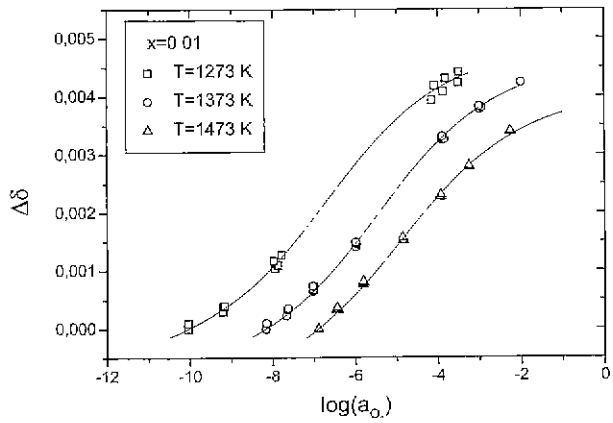

Fig. 2. Changes of the non-stoichiometry, $\Delta\delta=\delta-\delta_0$, in $(Ni_{1-x}Fe_x)_{1-\delta}O$ (x=0.01) as a function of the oxygen activity, ao_2, for T=1273 K, 1373 K and 1473 K (Open symbols : thermogravimetric measurements. Straight lines : values calculated with model 8).

corresponding quantities after the change in the oxygen activity. Only changes of the non-stoichiometry relative to an unknown reference value, δ_0, at the starting oxygen activity (reference point) can be measured:

$$\delta_n-\delta_0=\sum_{k=1}^{n}\Delta\delta_k \qquad \Delta\delta_k=\delta_k-\delta_{k-1}=\frac{b_k}{a_{k-1}} \qquad (2)$$

The results of the measurements are shown in Figs. 2 to 5 (open symbols; the experimental error is smaller than the symbol size) as a plot of $\Delta\delta=\delta-\delta_0$, versus oxygen activity, ao_2. We note that at constant temperature the observed changes $\Delta\delta$ increase with the oxygen activity while at constant oxygen activity they decrease with increasing temperature. Our results at 1273 K are in good agreement with the previously mentioned data obtained by coulometric titration at 1273 K in the same system.[5]

III. Modelling of the non-stoichiometry

1. Defect Models

In order to model the non-stoichiometry in the system $(Ni_{1-x}Fe_x)_{1-\delta}O$ we assume that NiO forms an inert, defect free matrix in which iron oxide is dissoved. Thus, all defects and also the non-stoichiometry in the doped oxide are due to the dopant iron. This assumption is very reasonable since the non-stoichiometry in pure NiO is by far smaller than the non-stoichiometry in the isostructural iron oxide $Fe_{1-\delta}O$ (see Introduction). Using the Kröger-Vink notation the most simple defects in the doped oxide are formed by oxidation of substitutional divalent iron, Fe_{Ni}^{x}, resulting in trivalent iron, $Fe_{Ni}^{\cdot}$, and cation vacancies V_{Ni}'':

$$2Fe_{Ni}^{x}+\frac{1}{2}O_2(g)\rightleftarrows 2Fe_{Ni}^{\cdot}+V_{Ni}''+O_O^{x} \qquad (3)$$

The law of mass action for the oxidation reaction in Eq. (3) reads:

$$K_V = \frac{[Fe_{Ni}^{\bullet}]^2 [V_{Ni}'']}{[Fe_{Ni}^{x}]^2 p_{O_2}^{1/2}} \quad (4)$$

Because in $Ni_{1-\delta}O$ and $Fe_{1-\delta}O$ the oxygen sublattice is perfect (compared to the cation sublattices) we have assumed in Eq. (4) that in $(Ni_{1-x}Fe_x)_{1-\delta}O$ the oxygen sublattice is also perfect, i.e. $[O_O^x]=1$. It is also possible that defect associates are formed as a consequence of coulomb interactions between the defects (see for example[7]). The most simple associates can be formed by trivalent iron, $Fe_{Ni}^{\bullet}$, and vacancies, V_{Ni}'', resulting in pairs, $P'=\{Fe_{Ni}^{\bullet}, V_{Ni}''\}$, or triplets, $T^x=\{Fe_{Ni}^{\bullet}, V_{Ni}'', Fe_{Ni}^{\bullet}\}^x$:

$$Fe_{Ni}^{\bullet} + V_{Ni}'' \rightleftarrows P' \qquad 2Fe_{Ni}^{\bullet} + V_{Ni}'' \rightleftarrows T^x \quad (5)$$

$$K_P = \frac{[P']}{[Fe_{Ni}^{\bullet}][V_{Ni}'']} \qquad K_T = \frac{[T^x]}{[Fe_{Ni}^{\bullet}]^2 [V_{Ni}'']} \quad (6)$$

Guided by the experiments and the modelling in wüstite, $Fe_{1-\delta}O$, higher and more complicated aggregates containing iron interstials are also possible,[8-11] e.g., the so-called Roth-cluster, $R'=\{Fe_i^{3\bullet}, 2V_{Ni}''\}'$, consisting of one trivalent iron interstitial, $Fe_i^{3\bullet}$, and two vacancies, V_{Ni}'', or the (4:1)-cluster, $C^{m'}=(Fe_i^{3\bullet}, 4V_{Ni}'')^{5'}$, consisting of one trivalent iron interstitial surrounded tetrahedrally by four cation vacancies. Particularly the latter defect complex has a high binding energy (in pure wüstite) according to atomistic simulations of Catlow and Stoneham.[12] Since isolated iron interstitials are not expected to be stable in the cubic close packed structure[13] we formulate the formation reactions for the Roth-cluster and the (4:1)-cluster without isolated iron interstitials:

$$Fe_{Ni}^{\bullet} + V_{Ni}'' + V_i^x \rightleftarrows R' \qquad K_R = \frac{[R']}{[Fe_{Ni}^{\bullet}][V_{Ni}''](2-[C^{m'}]-[R'])} \quad (7)$$

Concernig the (4:1)-cluster, $C^{m'}=\{Fe_i, 4V_{Ni}\}^{m'}$, we allow the cluster charge, m, to differ from the normal value in wüstite, m=5, resulting in:

$$(6-m)\,Fe_{Ni}^{\bullet} + 3V_{Ni}'' + V_i^x \rightleftarrows C^{m'} + (5-m)\,Fe_{Ni}^{x} \quad (8)$$

$$K_C = \frac{[C^{m'}][Fe_{Ni}^{x}]^{(5-m)}}{[Fe_{Ni}^{\bullet}]^{(6-m)}[V_{Ni}'']^3(2-[C^{m'}]-[R'])} \quad (9)$$

Eventually, the charge balance and the mass balance for iron read:

$$[Fe_{Ni}^{\bullet}] = 2[V_{Ni}''] + [P'] + [R'] + m[C^{m'}] \quad (10)$$

$$[Fe]_{total} = x(1-\delta) = [Fe_{Ni}^{x}] + [Fe_{Ni}^{\bullet}] + [P'] + 2[T^x] \quad (11)$$

Finally, the non-stoichiometry, δ, is given by:

$$\delta = [V_{Ni}''] + [P'] + [T^x] + [R'] + 3[C^{m'}] \quad (12)$$

In this defect model the 5 equilibrium constants, K_V, K_P, K_T, K_R, and K_C, and the cluster charge m are unknown parameters describing the defect structure of Fe-doped NiO. To limit the number of parameters we do not consider all defects but only the neutral structure elements Ni_{Ni}^{x} and Fe_{Ni}^{x} and between the charged defects the majority defects. If we allow at first only two oppositely charged defects we end up with 4 simple defect models (see Eq.(10)), where $Fe_{Ni}^{\bullet}$ is compensated either by V_{Ni}'', P', R' or $C^{m'}$. The next and more complicated class of defect models then consists of $Fe_{Ni}^{\bullet}$ as the only positively charged defect and two other defects, e.g. V_{Ni}'' and P' or V_{Ni}'' and T^x. The next class consists of $Fe_{Ni}^{\bullet}$ and three other defects, and so on. A list of the models considered in this paper can be found in Table 1. By fitting the calculated change in non-stoichiometry, $\Delta\delta_{model}$, to the measured value, $\Delta\delta_{exp}$ we obtain the most simple defect model describing the defect structure of Fe-doped NiO. Of course, this result is not unique, the real defect structure may be much more complicated or the set of chosen defects may have been wrong.

Table 1. Models for the Defect Structure in $(Ni_{1-x}Fe_x)_{1-\delta}O$.

	V_{Ni}''	P'	R'	$C^{m'}$
Ni_{Ni}^{x}, Fe_{Ni}^{x}, $Fe_{Ni}^{\bullet}$	model 1	model 2	model 3	model 4
	V_{Ni}'', P'	V_{Ni}'', T^x	V_{Ni}'', R'	V_{Ni}'', $C^{m'}$
Ni_{Ni}^{x}, Fe_{Ni}^{x}, $Fe_{Ni}^{\bullet}$	model 5	model 6	model 7	model 8

2. Results and Discussion

None of the simple models 1-4 can describe the measured non-stoichiometry, $\Delta\delta_{exp}$ since all 4 models yield too small slopes of $\Delta\delta_{model}$ as a function of a_{O_2}. Within the next class of models, models 5-8, consisting of three charged majority defects, only model 8 is able to fit the experimental data well (see Figs. 2-5, solid curves). Therefore we assume this model to represent the defect structure of Fe-doped NiO. As stated before, the real defect structure may be much more complicated, i.e. consist of more defects, but model 8 is the most simple model fitting the experimental data.

Model 8 consists of the neutral structure elements Ni_{Ni}^{x} and Fe_{Ni}^{x}, trivalent substitutional iron ions, $Fe_{Ni}^{\bullet}$, cation vacancies, V_{Ni}'', and (4:1)-clusters, $C^{m'}$. This means that the two equilibrium constants K_V and K_C and the cluster

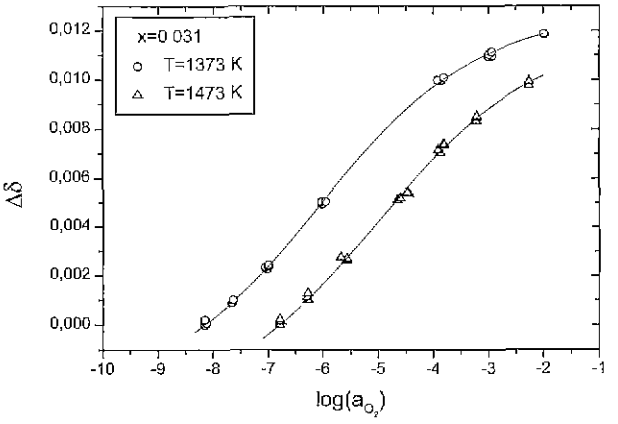

Fig. 3. Changes of the non-stoichiometry, $\Delta\delta=\delta-\delta_0$, in $(Ni_{1-x}Fe_x)_{1-\delta}O$ (x=0.031) as a function of the oxygen activity, a_{O_2}, for T =1373 K and 1473 K (Open symbols : thermogravimetric measurements. Straight lines : values calculated with model 8).

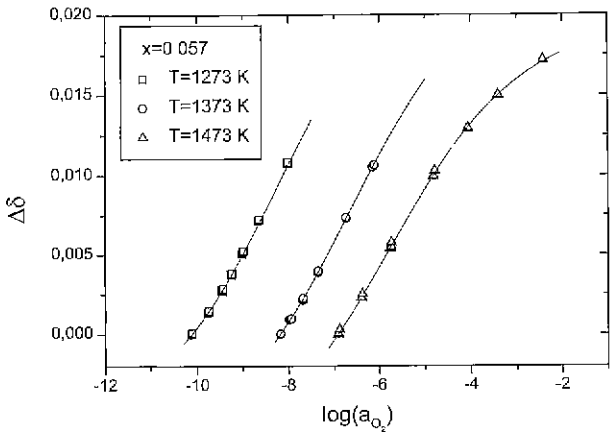

Fig. 4. Changes of the non-stoichiometry, $\Delta\delta=\delta-\delta_0$, in $(Ni_{1-x}Fe_x)_{1-\delta}O$ (x=0.057) as a function of the oxygen activity, a_{O_2}, for T=1273 K, 1373 K and 1473 K (Open symbols : thermogravimetric measurements. Straight lines : values calculated with model 8).

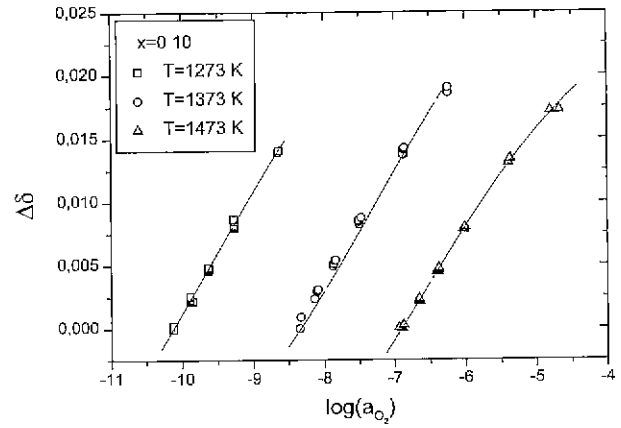

Fig. 5. Changes of the non-stoichiometry, $\Delta\delta=\delta-\delta_0$, in $(Ni_{1-x}Fe_x)_{1-\delta}O$ (x=0.10) as a function of the oxygen activity, a_{O_2}, for T=1273 K, 1373 K and 1473 K (Open symbols : thermogravimetric measurements. Straight lines : values calculated with model 8).

charge m have to be determined by a non-linear least-squares fitting procedure. Surprisingly we obtain for the cluster charge m=4±0.1, independent of temperature and dopant level. In contrast, the original (4:1)-cluster in $Fe_{1-\delta}O$, consisting of a trivalent iron interstitial and four cation vacancies, is five times negatively charged. Our result for the cluster charge m=4 in Fe-doped NiO can be interpreted as follows. The additional positive charge on the cluster (oxidation by one electron hole) may be located on Fe in the center of the cluster or on Ni or O on peripheral positions of the cluster, resulting in tetravalent interstitial iron, $Fe_i^{4\cdot}$, or trivalent nickel, $Ni_{Ni}^{\cdot}$, or monovalent oxygen, $O_o^{\cdot}$. Trivalent nickel, $Ni_{Ni}^{\cdot}$ can be excluded as majority defect since the cluster fractions reach high values (up to 1%) and it seems unprobable to have such high fractions of Ni^{3+}. Monovalent oxygen, $O_o^{\cdot}$, was excluded by Springhorn and Schmalzried[14] as a result of electrical conductivity measurements in Fe-doped NiO. This interpretation was supported by band structure calculations in the same material.[15] We conclude therefore that the (4:1)-cluster in Fe-doped NiO consists of tetravalent interstitial iron, $Fe_i^{4\cdot}$, and four cation vacancies, V_{Ni}'', in total being four times negatively charged. These experimental findings are in agreement with theoretical studies of Grimes *et al.*[13] who found that in NiO (4:1)-clusters with a tetrahedral iron ion have a high stability which is comparable to the stability of (4:1)-clusters in pure wüstite.

The results for the equilibrium constants, K_V and K_C, are shown in Figs. 6 and 7. Both constants depend on the iron fraction, x, (see Fig. 6) and the temperature dependence of the equilibrium constants follows no simple Arrhenius-behaviour (see Fig. 7). Both facts may indicate strong defect interactions in the doped oxide. In

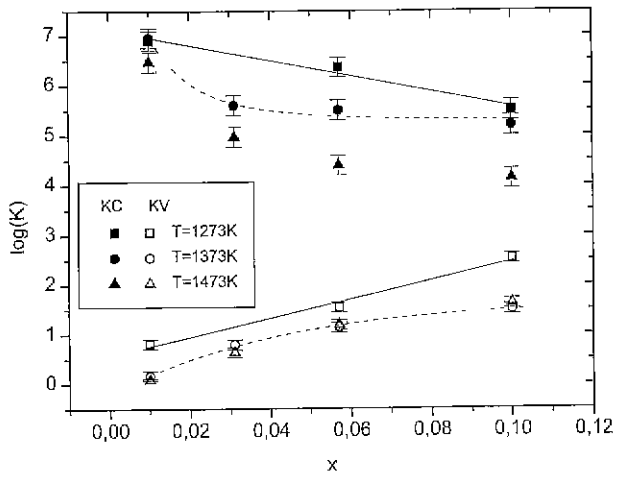

Fig. 6. Equilibrium constants K_V and K_C as a function of the iron fraction, x (the lines are only a guide to the eye).

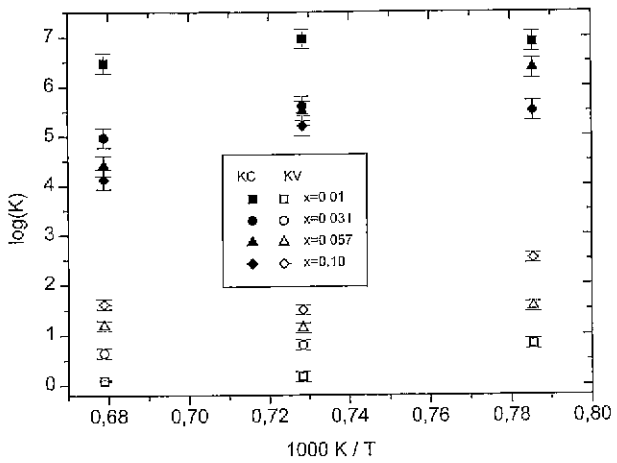

Fig. 7. Equilibrium constants K_V and K_C as a function of temperature, T (the lines are only a guide to the eye).

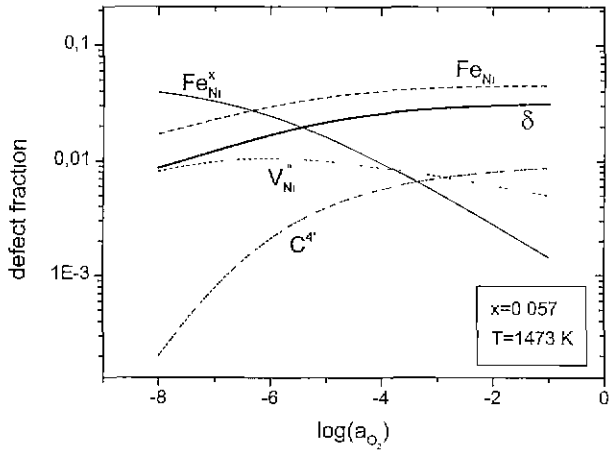

Fig. 8. Defect fractions in $(Ni_{1-x}\ Fe_x)_{1-\delta}O$ as a function of the oxygen activity, a_{O_2}(x=0.057, T=1473 K)

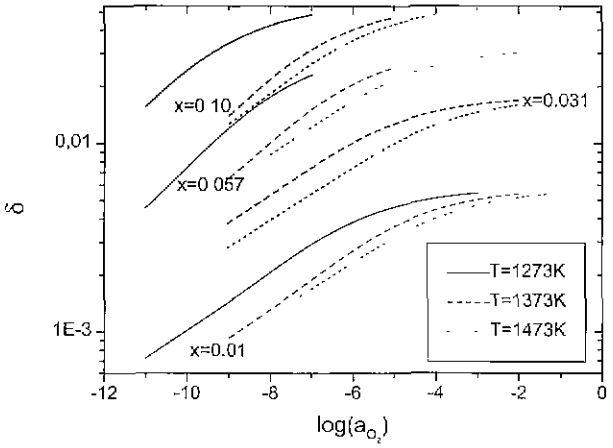

Fig. 9. Absolute values of the non-stoichiometry in $(Ni_{1-x}\ Fe_x)_{1-\delta}O$ as a function of the oxygen activity, a_{O_2}, for different iron fractions, x, and temperatures, T

our treatment in section III-1 we have used ideal laws of mass action, but we can consider the equilibrium constants to include activity coefficients, as a result of which the reaction enthalpies may depend on x and T.

With the knowledge of the equilibrium constants all defect fractions in $(Ni_{1-x}Fe_x)_{1-\delta}O$ can be calculated as a function of a_{O_2}, T and x. An example is shown in Fig. 8, demonstrating that at low a_{O_2} substitutional trivalent iron, $Fe_{Ni}^{\cdot}$, and cation vacancies, $V_{Ni}^{"}$, are the majority defects while $Fe_{Ni}^{\cdot}$, $V_{Ni}^{"}$ and (4:1)-clusters, C", dominate at high a_{O_2}. Absolute values for the non-stoichiometry, δ, are shown in Fig. 9. The nonstoichiometry increases at constant a_{O_2} and T with the iron fraction x while it decreases with increasing temperature at constant a_{O_2} and x. At high oxygen activities the non-stoichiometry reaches a saturation value, i.e. nearly all iron is oxidised to Fe^{3+} or Fe^{4+}. This is shown in Fig. 10 where the fractions of Fe^{2+}, Fe^{3+} and Fe^{4+} are shown as a function of the oxygen activity.

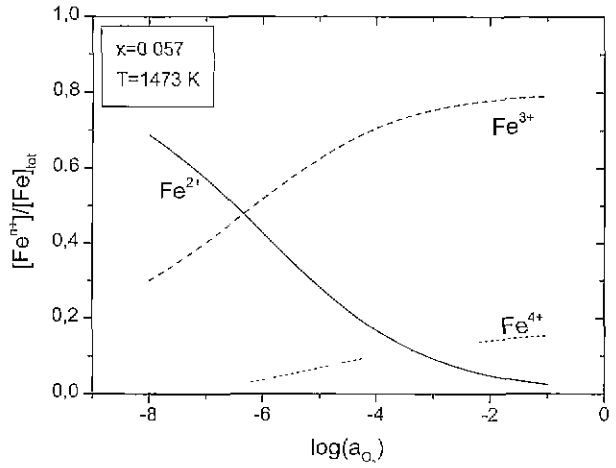

Fig. 10. Fractions of Fe^{2+}, Fe^{3+} and Fe^{4+} in $(Ni_{1-x}\ Fe_x)_{1-\delta}O$ as function of the oxygen activity, a_{O_2}, (x=0.057, T=1473 K).

IV. Summary

In Fe-doped nickel oxide, $(Ni_{1-x}Fe_x)_{1-\delta}O$, we have measured changes of the non-stoichiometry, Δδ, by thermogravimetry for four dopant fractions, x=0.01, 0.031, 0.057 and 0.10 and three temperatures, T=1273, 1373 and 1473 K. The obtained data can be modelled by a defect structure in which substitutional trivalent iron ions, $Fe_{Ni}^{\cdot}$ are compensated by cation vacancies, $V_{Ni}^{"}$, and (4:1)-clusters. These clusters are four times negatively charged and consist of tetravalent interstitial iron, $Fe_i^{4\cdot}$, surrounded tetrahedrally by four cation vacancies.

Acknowledgement

Financial support by the Fonds der Chemischen Industrie is gratefully acknowledged.

References

1. L.S. Darken, R.W. Gurry, "The System Iron-Oxygen. I. The Wüstite Field and Related Equilibria", *J. Am. Chem. Soc.*, **67**, 1398-1412 (1945).
2. M. Keller, R. Dieckmann, "Defect Structure and Transport Properties of Manganese Oxides (I): The Non-stoichiometry of Manganosite ($Mn_{1-\delta}O$)", *Ber. Bunsenges. Phys. Chem.*, **89**, 883-893 (1985).
3. R. Dieckmann, "Cobaltous Oxide Point Defect Structure and Non-Stoichiometry, Electrical Conductivity, Cobalt Tracer Diffusion", *Z Phys. Chem. NF*, **107**, 189-210 (1977).
4. N.L. Peterson, C.L. Wiley, "Point Defects and Diffusion in NiO", *J. Phys. Chem Solids*, **46**, 43-52 (1985).
5. F. Schneider, H. Schmalzried, "Thermodynamic Investigation of the System Ni-Fe-O", *Z. Phys. Chem. NF*, **166**, 1-18 (1990).
6. R. Dieckmann, "Defects and Cation Diffusion in Magnetite (IV): Nonstoichiometry and Point Defect Structure

of Magnetite ($Fe_{3-\delta}O_4$)", *Ber Bunsenges. Phys. Chem.*, **86**, 112-118 (1982).
7. R. Schmackpfeffer, M. Martin, "Tracer Diffusion and Defect Structure in Ga-doped CoO", *Phil. Mag. A*, **68**, 747-765 (1993).
8. F. Koch, J.B. Cohen, "The Defect Structure of $Fe_{1-x}O$", *Acta Cryst. B.*, **25**, 275-287 (1969).
9. J. Nowotny, M. Rekas, "Defect Structure and Thermodynamic Properties of the Wüstite Phase ($Fe_{1-y}O$)", *J. Am. Cer. Sec.*, **72**, 1221-1228 (1989).
10. S. Tomlinson, C. Catlow, J. Harding, "Computer Modelling of the Defect Structure of Non-Stoichiometric Binary Transition Metal Oxides", *J. Phys. Chem. Solids*, **51**, 477-506 (1990).
11. W. Schweika, A. Hoser, M. Martin, A.E. Carlsson, "The Defect Structure of Ferreous Oxide $Fe_{1-x}O$", *Phys. Rev. B.*, **51**, 15771-15788 (1995).
12. C.R.A. Catlow and A.M. Stoneham, "Defect Equilibria in Transition Metal Oxides", *J Am. Ceram. Sec.*, **64**, 234-236 (1981).
13. R.W. Grimes, A.B. Anderson, A.H. Heuer, "Interaction of Dopant Cations with 4:1 Defect Clusters in Non-Stoichiometric 3d-Transition Metal Monoxides: A Theoretical Study", *J. Phys. Chem. Solids*, **48**, 45-50 (1987).
14. C. Springhorn, H. Schmalzried, "The Electronic Conduction Mechanism of NiO-Crystals", *Ber Bunsenges. Phys Chem.*, **98**, 746-748 (1994)
15. W.C. Mackrodt, "The Nature of Valence Band Holes in Pure and Fe-Doped NiO: An ab initio Hartree-Fock Study", *Ber. Bunsenges. Phys. Chem.*, **101**. 169-175 (1997).